

# Synthesis and characterization of microcrystalline and nanocrystalline cellulose from cotton linter for composite applications

Sohana Pervin, S. M. Abdur Razzaque, G. M. Arifuzzaman Khan,  
Shamsul Alam, Moshir Rahman\*

*Polymer Research Laboratory, Department of Applied Chemistry and Chemical Engineering  
Islamic University, Kushtia-7003, Bangladesh*

\*Email: [drmrhaniuk@gmail.com](mailto:drmrhaniuk@gmail.com)

Received: 16 July 2023; Accepted for publication: 25 December 2023

**Abstract.** In this work, microcrystalline cellulose (MCC) and nanocrystalline cellulose (NCC) was synthesized from cotton linter collected from a textile mill in Bangladesh. The synthesis was carried out through several steps; alkali treatment,  $\text{NaClO}_2$  bleaching and acid hydrolysis. The acid hydrolysis was conducted with 9N and 12N sulphuric acid ( $\text{H}_2\text{SO}_4$ ) for synthesis of MCC and NCC, respectively. The raw and synthesized samples were characterized by measuring bulk density, FTIR, SEM and WAXD techniques. The bulk density of MCC and NCC is higher than that of the raw sample, due to shorter chain length, diameter and reduction of amorphous region of cellulose chain. The oxidation reaction took place during the MCC and NCC preparation was detected by FTIR spectra. From the SEM images, it is seen that the surface of untreated sample looks relatively smooth as compared to the rough surface of treated samples due to voids formation and absence of wax on the surface. The crystallinity index of MCC and NCC was measured from the peaks at  $14.6^\circ$  and  $22.6^\circ$  ( $2\theta$  angles) of WAXD curves. It shows the enrichment in the proportion of crystalline cellulose in MCC. The thermal stability of the MCC is better than that of other experimented samples. Finally, the synthesized MCC and NCC may be emerging and promising materials with exceptional properties.

**Keywords:** cotton linter, acid hydrolysis, microcrystalline cellulose, nanocellulose, bulk density, crystallinity

**Classification numbers:** 2.9.3, 2.9.4, 2.10.2, 2.10.3, 3.3.2.

## 1. INTRODUCTION

In recent years, much more attention has been paid to the sustainable, green and environmental friendly materials because of the increasing public interest in environmental issues and growing pressure from legislative institutions [1 - 2]. Due to their unique characteristics viz. biodegradability and renewability, low cost as well as low carbon dioxide

release cellulose materials have been categorized as sustainable, green and environmental friendly materials. Cellulose is a linear branched polysaccharide. It is produced from  $\beta$ -glucose monomers linked by 1 - 4 glycosidic bonds with degree of polymerization ranges from 10000 to 15000 [3]. Cellulose is a multifunctional raw material which can be self-assembled into well-defined architectures at multiple scales from nano to micro-size and is expected to be able to replace many non-renewable materials [4]. Cotton is an important source of cellulose. It is normally used in textile industry as medium length fibers ranges between 18 and 28 mm long. In contrast, the shorter cotton linter fiber is generally known as cotton linter cellulose (CLC) obtained from textile and garment industry as waste material. Therefore, it can be deemed suitable for the extraction of micro and nanocellulose. In general terms, it is proved for effective use in many purposes, whether it is colored or not, despite some differences in yield, in sulfonation efficiency and thermal stability [5]. More specifically, a study on the extraction of MCC and NCC from cotton linter originating from Bangladesh did demonstrate that controlling waste stream for extraction may result in a more uniform quality product: cotton linter is particularly adapted, because it does not require pulping before extraction. At present, cotton linter is considered as a valuable raw material for cellulose based industry. It has been used for making absorbent cotton, special papers, cellulose nitrate and acetate [6]. Rahman *et al.* have prepared MCC from cotton linter [7]. Now it is also used in advanced industrial purposes such as a novel sulfonic-cellulose succinate half ester dispersant for coal-water slurry was successfully synthesized using cotton linters [8]. In Bangladesh, there are about 5,700 textile industries which produce a lot of cotton linter every year. Some of them are used directly as tattered cloths and sometimes found in application in pillow or bed mattress making. In a word, it has no any value added application in Bangladesh. Therefore, it is crying need to accumulate such huge amount of this textile byproduct and find profitable applications. Extraction of microcrystalline and cellulose nanocrystals from textile wastes represent an important way of upcycling it, therefore obtaining a material with some value, hopefully with a reasonable yield that would make the extraction worthwhile. The extraction of MCC and NCC has been performed from this textile waste obtained from the production systems using different natural fibers, with the idea of operating as much as possible in conditions of circular economy; the using a zero waste strategy [9]. But even today it is still a challenge to isolate MCC and NCC at a reasonable cost with low degradation and to disperse them evenly in polymer matrixes. However, many methods, viz. chemical and mechanical method have been employed to generate MCC and NCC for using in bio-nanocomposites followed by film casting as well as freeze dry compressive molding and extrusion. Chemical processes were frequently practiced due to easy and quick extraction, low cost and to obtain the lowest shortest fiber diameter. Cellulose nanocrystals can be generated by chemical treatment, especially acid hydrolysis from various biomass resources [10]. Mandal and Chakrabarty [11] isolated more crystalline nanocellulose by acid hydrolysis from sugarcane bagasse by acid hydrolysis of native cellulose fiber using a concentrated inorganic acid commonly sulfuric or hydrochloric acid. Abrahama *et al.* [12] also tried to extract nanocellulose by steam explosion technique along with mild chemical treatment. Recently some researchers adopted ultrasonic [13] and enzymatic pre-treatment methods [14] for the preparation of nanofibres. Cheng Q. *et al.* [15] produced cellulose fibrils in micro and nano-scales from several cellulose sources, including regenerated cellulose fiber, pure cellulose fiber and microcrystalline cellulose by ultrasonic treatment to reinforce PVA to make biodegradable nanocomposites by film casting technique. NCC can be used as fillers in composites [16-19] because they have interesting mechanical properties [18]. Due to small size, high surface area, insolubility in water and high aspect ratio, MCC is a promising reinforcing material of biocomposites. Composites from MCC reinforced with various polymer provide strength,

rigidity and biodegradability, as already reported [20 - 22]. Rahman *et al.* in their study; fabricated MCC-UF (urea formaldehyde) composites and showed that the thermal stability as well as mechanical properties of MCC-UF composite is better than those of other CLC-UF composites [7]. There is a great number of potential applications of nanocellulose within different industries including composites for construction [23 - 24]. Wei Li *et al.* prepared a magnetic composite using nanocellulose fiber as matrix [25]. Cellulose nanofibres have been shown to be useful for generating hierarchical composites because it offers a way for long micrometer sized fiber to be more effectively used in composites by enhancing coupling between the fiber surface and the surrounding resin [26].

This research is focused on the synthesis of MCC and NCC by acid hydrolysis from CLC and their characterization. Because, nanocellulose is a new frontier subject of research owing to its unique material properties [27]. The use of strong acids with high concentration (70-80%) for the preparation of MCC and NCC from CLC tend to be toxic and the degradation of cellulose. We used sulfuric acids with mild concentration which overcome toxicity with no degradation of cellulose. Here we report on an efficient extraction of MCC and NCC from CLC by a mild chemical treatment. The structural arrangement, intermolecular interaction and chemical functional groups in the cellulose micro and nanocrystals were characterized by FTIR comparing with  $\alpha$ -cellulose of raw CLC. The morphological change was characterized by SEM analysis. Thermal behavior was characterized by TGA measurement. The bulk densities of the samples were also measured. However, the present research work concentrates on the feasibility of the extraction method and the physico-chemical properties of MCC and NCC obtained using present technique.

## **2. MATERIALS AND METHODS**

### **2.1. Materials**

In this research work, cotton linter is used as a source of cellulose for the synthesis of MCC and NCC. Generally, waste cotton linter is obtained as a byproduct from textile mills and garment factories. It was collected from Imran Textile Industry, Pabna, Bangladesh. All the chemicals used in the present investigation were analytical reagent grade purchased from Sigma Aldrich.

### **2.2. Methods**

#### *2.2.1. Scouring of CLC*

The removal of impurities such as dirty materials and other gummy substances from textile cotton linter is called scouring. It was carried out by the use of surface active agents like soda and detergents. CLC was scoured in a solution containing 6.5 g of jet powder and 3.5 g of soda per liter of distilled water at 70 - 75 °C for 30 minutes in a large beaker. The ratio of the CLC to solution was 1:50 (w/v). After scouring, the CLC was thoroughly washed with distilled water for several times and dried in open air and finally stored in desiccator.

#### *2.2.2. Alkali Treatment of Scoured CLC*

The alkali treatment of scoured CLC was carried out by using 17.5 % NaOH solution. The scoured CLC was scoured in 17.5 % NaOH solution at 40 °C for 4 hours in a large beaker heated by a heating mantle. The ratio of the fiber to solution was 1:50 (w/v). After treatment, the CLC

was thoroughly washed with 2.0 % glacial acetic acid for three times to make it neutral. Finally, it was washed with distilled water, dried in open air and stored in desiccator.

### 2.2.3. Bleaching of Alkalized CLC

Bleaching of mercerized CLC was carried out by using 0.7 %  $\text{NaClO}_2$  solution. Mercerized CLC was poured in 0.7 %  $\text{NaClO}_2$  solution at  $90^\circ\text{C}$  for 90 minutes in a large beaker heated by a heating mantle. The ratio of the CLC to solution was 1:50 (w/v) and the pH of the solution was adjusted at 4 by acetic acid and sodium acetate buffer solution. The maintaining of this pH is very necessary, because many organic acids are liberated during bleaching and pH of the medium would be changed. After bleaching, the fiber was thoroughly washed with distilled water for several times and then 0.2 % sodium metabisulphite solution. Finally, it was washed with distilled water, dried in open air and stored in desiccator.

### 2.2.4. Acid Hydrolysis of Bleached CLC

The CLC as obtained from bleaching was acid hydrolyzed by refluxing with 9N and 12N sulfuric acid. 9N and 12N sulfuric acid solutions were used for the synthesis of MCC and NCC, respectively. For the synthesis of both, 10 g of bleached CLC was added in each of the mentioned sulfuric acid solution. The CLC to liquor ratio was maintained at 1:50 (w/v). Then the obtained suspension were then placed on a magnetic stirrer and stirring was continued up to 6 hours using a magnetic bar. After acid hydrolysis, the forming white powder was filtered and thoroughly washed with distilled water. Finally, the sonication of the white powder was performed in an ultrasonic bath for 12 hours.

## 2.3. Characterization Techniques

### 2.3.1. Bulk Density Measurement

Bulk density is the mass of a dry sample per unit volume, i.e. mass of solid divided by the volume of the sample. In order to determine it, the tested specimen was prepared according to the ASTM C135-76 and can be calculated by the following formula:

$$\text{Bulk density, } D = W_s/V,$$

where,  $W_s$  = Weight of the tested sample, kg;  $V$  = Volume of the tested sample,  $\text{m}^3$ .

### 2.3.2. Fourier Transform Infrared Spectroscopy (FTIR) Measurement

The FTIR spectra of raw CLC and chemically treated CLC samples were recorded on an IR instrument (SHIMADZU IR Prestige-21, Japan) between the wavenumber ranges from 400-4000  $\text{cm}^{-1}$  with a resolution of 4  $\text{cm}^{-1}$ . The samples were ground into powder by a fiber microtome and then blended with KBr followed by pressing the mixture into ultra-thin pellets. The sample pellets were prepared by mixing approximately 0.5 mg of powder sample and 100 mg of dry KBr in a small mortar pestle.

### 2.3.3. Scanning Electron Microscopy (SEM) Analysis

SEM photographs of the surfaces of virgin CLC and treated CLC were captured using SEM technique (ZEISS SIGMA VP, USA). For this, the samples were coated with gold using the sputtering technique and magnifications 1000x, 5000x, 20000x and 50000x were taken for each sample. Particle size distribution (PSD) curves of these SEM images were also drawn by Image J and origin 8 software.

### 2.3.4. Wide-angle X-ray Diffraction (WAXD) Analysis

Wide-angle X-ray diffractogram pattern for raw and treated CLC was obtained by wide angle X-ray diffractometer (RIGAKU ULTIMA IV, Japan) using Cu K $\alpha$  radiation ( $\lambda = 0.154$  nm), voltage of 50 kV and current of 40 mA with  $2\theta$  ranges from 5 - 35° increased in step of 3°/min. The data was analyzed by origin 8 software.

### 2.3.5. Thermo Gravimetric Analysis (TGA)

Thermo gravimetric analysis was performed with Thermal Analyzer (TA) instrument (NETZSCH STA449F5, Germany) to study the thermal degradation behavior of the samples. The TGA apparatus was flushed with nitrogen atmosphere and 10 mg of sample was used. Each sample was heated from room temperature to 600°C with an increasing rate of 5°C/min, TGA and DTG curves were obtained.

## 3. RESULTS AND DISCUSSION

Different characteristic properties of raw CLC, synthesized MCC and NCC were investigated in this study. The results obtained from various experiments as shown in the following sections:

### Bulk Density

It has been evident that the bulk density of CLC, MCC and NCC are fairly different from each other. The average bulk density of the raw CLC is 1.01 g/cm<sup>3</sup>. The alkali treatment removes a certain amount of lignin, hemicellulose, wax and oils that cover the external surface of the fiber cell wall.

Table 1. Bulk density of raw CLC, Bleached CLC, MCC and NCC.

Name of Sample	No.of Exp.	Mass (g)	Volume (cm <sup>3</sup> )	Bulk Density (g/cm <sup>3</sup> )	Mean Bulk Density (g/cm <sup>3</sup> )
Raw CLC	1	5.05	5	1.01	1.01
	2	5.10	5	1.02	
	3	5.00	5	1.00	
Bleached CLC	1	7.55	5	1.55	1.54
	2	7.70	5	1.54	
	3	7.95	5	1.53	
MCC	1	10.05	5	2.01	2.01
	2	10.10	5	2.02	
	3	10.00	5	2.00	
NCC	1	10.45	5	2.09	2.08
	2	10.35	5	2.07	
	3	10.40	5	2.08	

During bleaching, it causes the complete elimination of the remaining cementing materials from the fiber. Hence, the percentage of lignin decreases from raw fiber to bleached fiber. The samples were further broken down into leaner fragments by the sonicator of acid hydrolysis [28]. As the data given in Table 1, the average bulk density of bleached CLC and MCC is higher than that of raw CLC. However, the bulk density of NCC is higher than that of CLC and MCC. It is happened due to shorter chain length, diameter and reduction of amorphous region in CLC. The bulk density of the banana peel cellulose is higher than that of the smaller particle sized commercial cellulose [29]. The results were similar to those reported by Prakhonpan *et al.* [30].

## FTIR Spectra

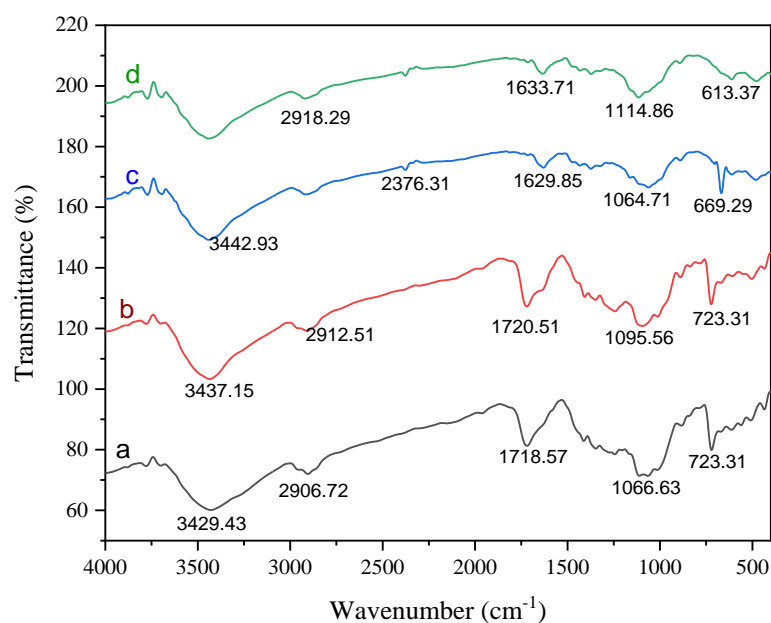


Figure 1. Superimposition curves of FTIR spectrum of (a) Raw CLC, (b) Bleached CLC, (c) MCC and (d) NCC.

Table 2. Infrared absorption wavenumbers of raw CLC, Bleached CLC, MCC and NCC.

Peak regions ( $\text{cm}^{-1}$ )	Absorption Bands
3570-3450	-OH bond stretching in alcohol
3000-2500	-OH bond stretching in cellulose
1730- 1715	C=O stretching of $\alpha$ , $\beta$ unsaturated esters
1725-1700	C=O stretching of saturated aliphatic acids
1715-1690	C=O stretching of aryl aldehyde
1620-740	C-H stretching of lignin
1350-1260	C-O stretching at primary alcohol present in guaiacyl lignin, cellulose and hemicellulose
1225-1000	Characteristic absorption of COH group
1250-1000	C-O of tertiary alcohol
1200-920	$\beta$ - glycosidic linkage of glucose ring of cellulose
Near 1100	C-O of secondary alcohol

Infrared transmittance spectra with main observed peaks of the tested samples are shown in the Fig. 1. Table 2 presents the analysis of the peaks along with their associated groups. The

FTIR spectrum of raw CLC contains the typical vibration bands of the components mainly corresponding to the cellulose, hemicellulose and lignin. The hydrophilic tendency of the cellulose and CLC are reflected in the broad absorption band at 3500 - 3000  $\text{cm}^{-1}$  region which is related to the hydroxyl (-OH) groups present in their main chain. Between 1600 - 900  $\text{cm}^{-1}$  region, it is clear that in CLC vibrations of chemical components of the lignin at wavenumber of 1514  $\text{cm}^{-1}$  for guaiacyl and 1428, 1372 and 1325  $\text{cm}^{-1}$  associated with syringyl. These absorptions are consistent with those of the typical cellulose backbone. The peak present at 1740-1730  $\text{cm}^{-1}$  in the spectrum corresponds to the raw cotton linter could be due to the presence of C=O linkage, a characteristic group of lignin and hemicellulose at 1765 - 1715  $\text{cm}^{-1}$ . Another possibility is that the carboxyl (-COOH) or aldehyde (-CHO) absorption could be arisen from the opened terminal glycopyranose rings or oxidation of the -CHO groups. Alkali treatment reduces the hydrogen bonding due to the removal of the hydroxyl groups by reacting with sodium hydroxide. This results in the increase of the -OH concentration, evident from the increased intensity of the peak between 3300 and 3500  $\text{cm}^{-1}$  bands compared to the untreated fibers [31 - 32].

Almost the same absorption peaks as shown in the cellulose fibers are observed in the spectrum of the MCC and NCC. This indicated that the structure of cellulose has not been damaged after the acid treatment [33]. On acid hydrolysis, the -OH group of cellulose is oxidized to aldehyde (-CHO) or carboxyl (-COOH) group giving the identical peak at 1736  $\text{cm}^{-1}$ . As the concentration of acid increases, the intensity of peak at 1736  $\text{cm}^{-1}$  of the samples increases. From the figure, it is observed that the very low intensity of the peak is negligible for CLC but it gradually increases in case of MCC and NCC. On the other hand, the peak centered at 1643  $\text{cm}^{-1}$  in the FTIR spectrum of CLC may be due to the C=O band of hemicellulose. The intensity of the peak decreases from cellulose to NCC as the hemicellulose is removed gradually by acid hydrolysis. From the FTIR analysis, it has been concluded that there is a reduction in the quantum of binding components present in the fibers due to the chemical treatment. The raw CLC gives the characteristic peaks in between 1740 - 1730  $\text{cm}^{-1}$  and 1300-1200  $\text{cm}^{-1}$ . The peaks are produced mainly for the presence of hemicellulose and lignin in the raw CLC. This type of characteristic peaks are completely absent in the final bleached and acid hydrolyzed CLC. The FTIR spectra of MCC and NCC are not massive different with cellulose. It indicates that no new bonds were formed during acid hydrolysis.

### **SEM Images**

The trend in size reduction during various processing steps is demonstrated with the help of SEM. Figures 2(A), 2(B) and 2(C) show the SEM micrographs and PSD curves of different tested samples. The diameter of the raw CLC fiber is much bigger and each fiber appears to be composed of several microfibrils. Each elementary CLC possesses a compact structure, exhibiting an alignment in the fiber axis direction. It also displays a lot of non-fibrous components scattered over the fiber surface. During digestion, the cuticle of the fibers is totally removed, the primary wall loses those parts which are soluble in caustic soda and the secondary walls with their screw structure and the 95 % of cellulose content are chemically attacked [34]. Acid treatment of bleached and alkali treated CLC helps in defibrillation of the fibrils where by the diameter of the fibrils is reduced to a greater extent, also possibly because of removal of non-cellulosic constituents as well as the CLC is breakdown into small particles. The SEM image of bleached CLC showed the intact cotton fiber devoid of any fibrillation.

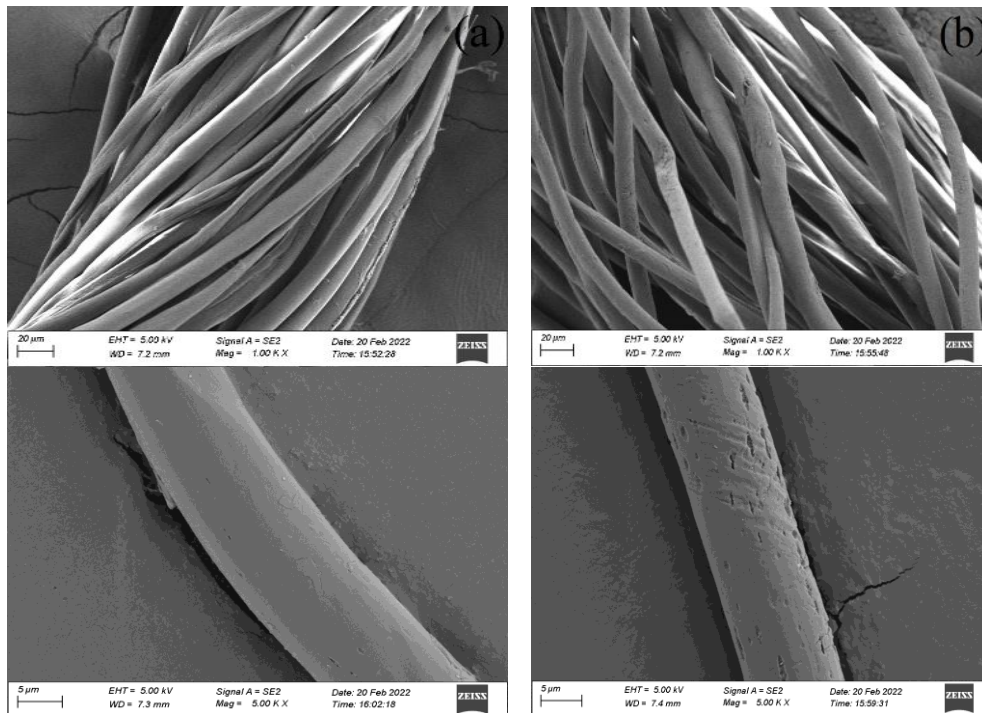


Figure 2(A). SEM images of: (a) Raw CLC (1000X and 5000X magnifications), and (b) Bleached CLC (1000X and 5000X magnifications).

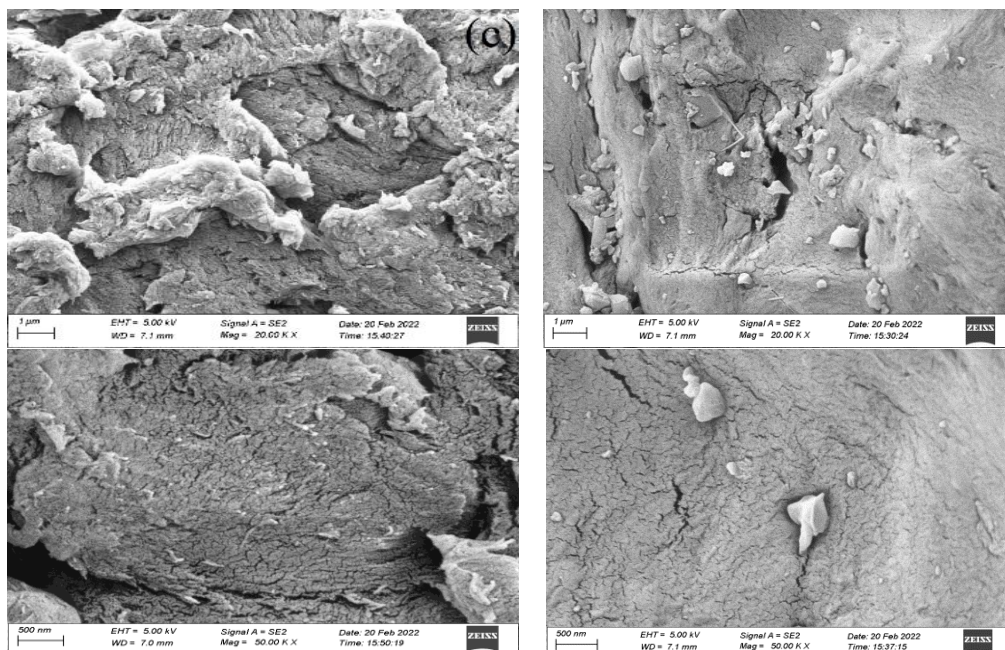


Figure 2(B). SEM images of: (c) MCC (20000X and 50000X magnifications), and (d) NCC (20000X and 50000X magnifications).



The initiation of fibrillation after the pulping stage and the extent of fibrillation increased significantly after the beating and refining processes [35]. From the SEM images, it is also seen that the surface of untreated sample (CLC) looks relatively smooth as compared to the rough surface due to voids and absence of wax on the surface of bleached CLC, MCC and NCC. This is similar with the microstructure of the commercial cellulose which is fibrous with a smooth surface and it has a fiber length about 200 - 300  $\mu\text{m}$  [29]. The size of pore on bleached CLC, MCC and NCC is increased due to removal of impurities. On acid hydrolysis, the surface of MCC and NCC looked rougher and created cavity due to completely removal of impurities. The microroughness of the surface is successfully developed on the fiber surface [36]. So, after chemical treatment, the surface of CLC changed noticeably.

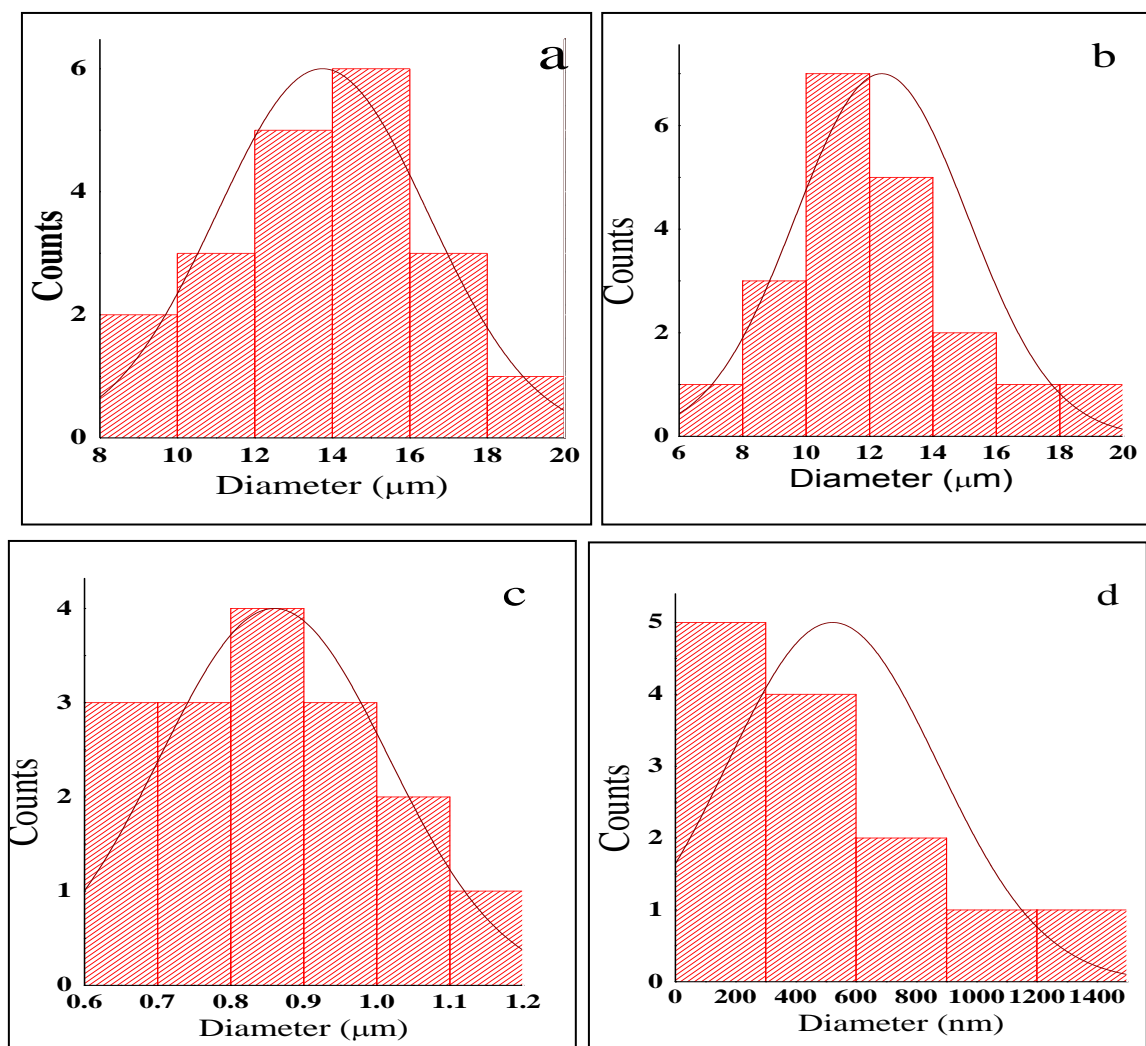


Figure 2(C). PSD curves of: (a) Raw CLC, (b) Bleached CLC, (c) MCC and (d) NCC.

The particle size distribution of a powder or granular material is a list of values or a mathematical function that defines the relative amount typically by mass of particles present according to size. PSD curves obtained from the SEM images showed the large variation in the particle size. The particles are in the range of 10 - 16  $\mu\text{m}$  with average diameter size of raw CLC

and bleached CLC (Figs. 2C (a), (b)). But in case of MCC and NCC the range of average diameter size is 0.8 - 1.0  $\mu\text{m}$  and 500 - 700 nm, respectively (Figs. 2C (c), (d)).

### WAXD Images

Figure 3 has shown the X-ray diffractogram of the investigated specimen which has been detected by WAXD. On removal of the noncellulosic constituents from the fibers by chemical treatment, the degree of crystallinity and crystallinity index will change. The fiber constitutes crystalline and amorphous regions. The degree of crystallinity, i.e., the amount of crystalline cellulose present in a cellulosic fiber cannot be exactly defined, as neither the crystalline portions are perfect crystals nor the non-crystalline portion completely disordered. The diffractogram of different CLC, MCC and NCC show two peaks around  $2\theta = 17.2^\circ$  (peak 1) and  $23.2^\circ$  (peak 2) which are typical peaks of cellulose I. Comparing with the bleached CLC, there is no crystalline transformation of the crystalline structure in the MCC samples due to invisible changes in the diffraction angle ( $2\theta$ ). It is also observed that after high concentrated acid (12 N) treatment the crystalline peak intensity at  $23.2^\circ$  of MCC was increased. The increase in the intensity indicated that the acid hydrolysis induced the crystallinity index (CrI %) due to the removal of amorphous materials like hemicellulose, lignin and some other non-cellulosic materials.

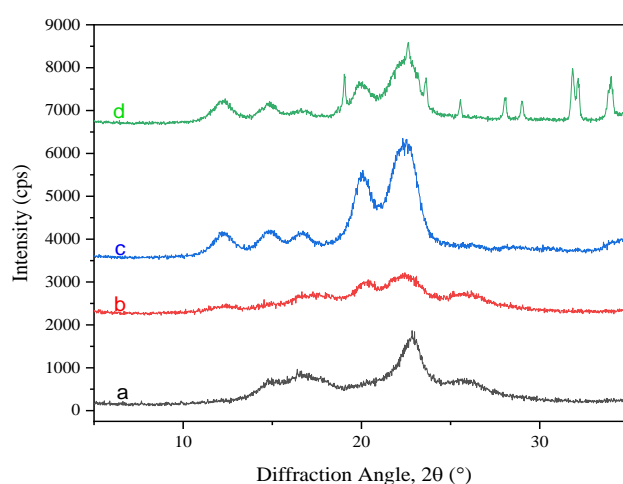


Table 3. Crystallinity index of different CLC, MCC and NCC.

Name of Sample	Crystallinity Index (%)
Raw CLC	68
Bleached CLC	72
MCC	80
NCC	78

Figure 3. Superimposition XRD curves of: (a) Raw CLC, (b) Bleached CLC, (c) MCC and (d) NCC.

It can be noted that the increased orientation of cellulose along a particular axis with the non-cellulosic polysaccharides which are removed by hydrolysis and the amorphous zones are dissolved. If the acid acts on cellulose microfibril surfaces, consuming the less ordered surface layers of cellulose, the internal ordered cellulose chains will become surface chains resulting in production of more amorphous cellulose and a further decrease in cellulose CrI [37]. It can also be noted that the peak intensity ratio between the peaks  $23.2^\circ$  and  $17.2^\circ$  are increased with the increase of acid concentration up to a maximum level then decrease. This may be due to higher acid concentration; degradation of cellulose occurs which may decrease the CrI in case of NCC (Table 3). Kanchanalai *et al.* showed that CrI of non-pretreated Avicel was approximately 56.7 % but a steep change in CrI observed in the narrow range of  $\text{H}_3\text{PO}_4$  concentration between 77 and 80 wt. % [38]. Morais *et al.* showed that the higher crystallinity is confirmed by the CrI which was 64.42 % for linter and 90.45 % for nanocellulose [5]. With the treatment of NaOH

and bleaching agents, the lignin is removed and in this case also the degree of crystallinity goes on increasing. This may be due to the removal of lignin which acts as a cementing material and on delignification, an ordered arrangement of the crystalline cellulose in the structure takes place [28]. The higher acid concentration produces NCC with lower crystallinity than MCC and it indicates that the addition of acid with higher concentration is not only to break the amorphous region of the cellulose but also damage the parts of crystalline structure. The hydrolysis with 9N sulfuric acid will break the amorphous region of CLC to produce MCC with higher CrI. However, when the used acid concentration is higher such as 12 N, the crystalline part can be damaged during hydrolysis consequently the CrI is decreased.

### Thermal Properties

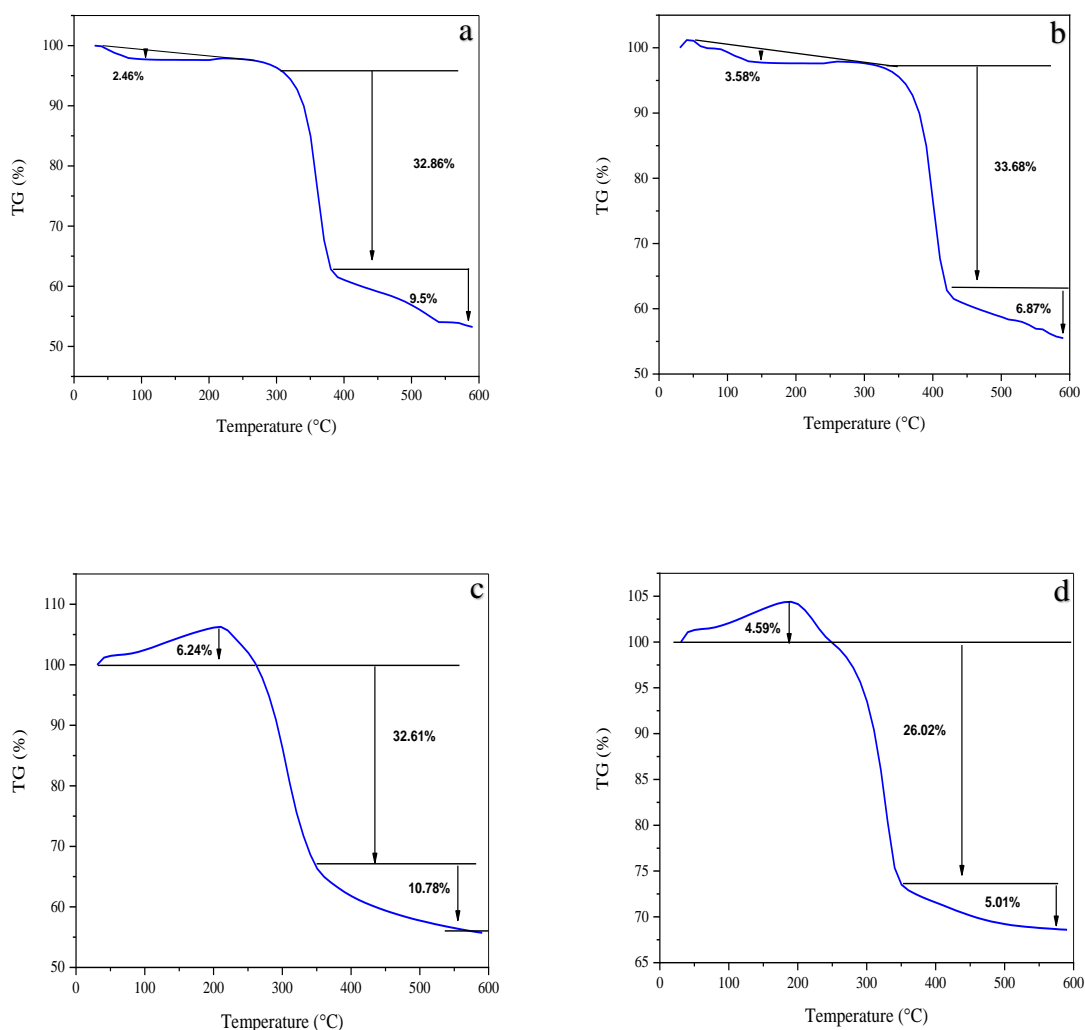


Figure 4. TG curves of: (a) Raw CLC, (b) Bleached CLC, (c) MCC and (d) NCC.

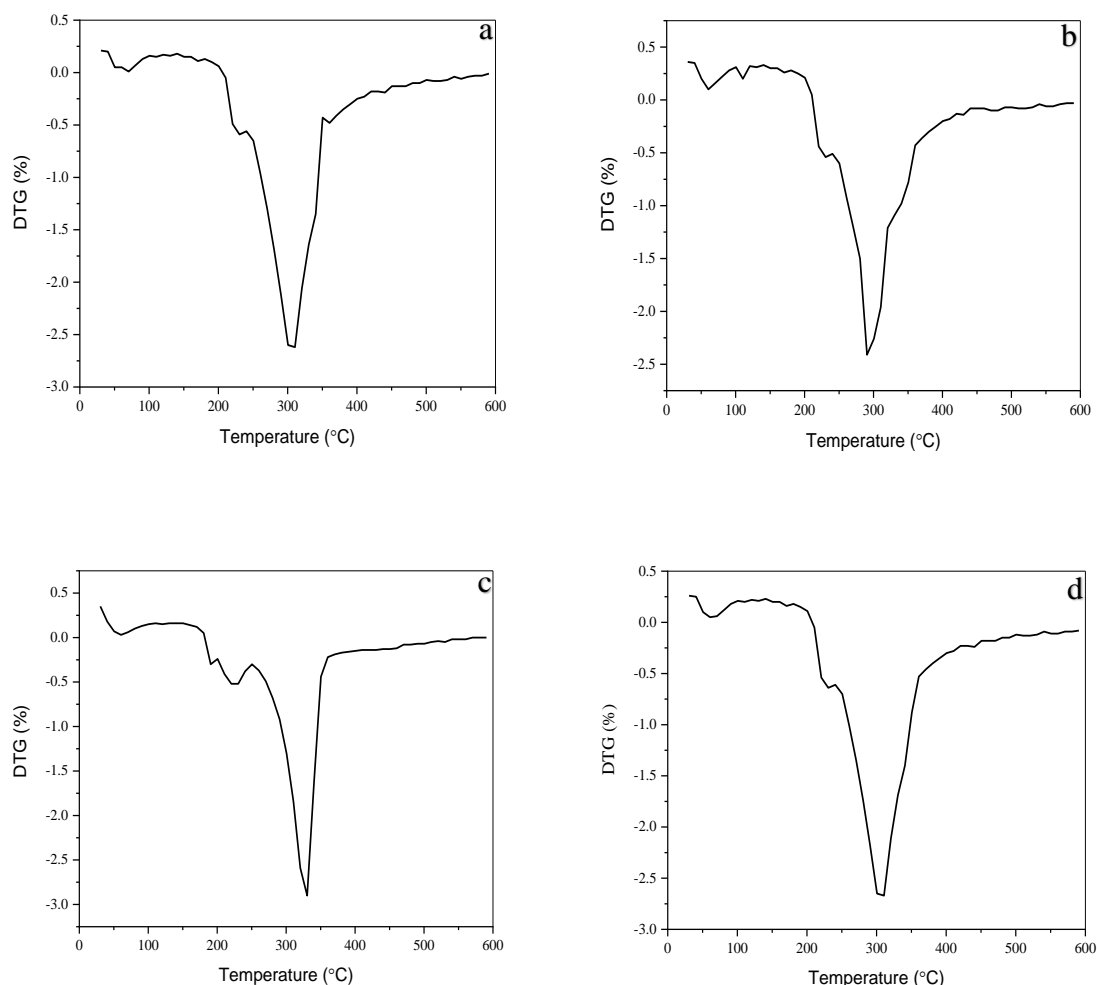


Figure 5. DTG curves of: (a) Raw CLC, (b) Bleached CLC, (c) MCC and (d) NCC.

The thermal behavior of raw CLC, bleached CLC, MCC and NCC could be determined from the TGA and DTG curves presented in Fig. 4 and Fig. 5 at an increasing heating rate of 5 °C/min. Due to the difference in the chemical structures among cellulose, hemicellulose and lignin; they usually decompose at different temperatures. Many studies related to the decomposition of lignocellulosic materials can be found in specific literature. For convincing explanation, four different temperature ranges, i.e. from 20 - 170, 171 - 270, 271 - 400 and above 400 °C, were considered on the basis of the degradation of the constituent of CLC, MCC and NCC. The first peak is occurred due to removal of moisture. Morais *et al.* showed that there is a small weight loss around 45 - 50 °C related to moisture [5]. The second peak is occurred due to the removal of low molecular weight substances and third peak is occurred due to cellulose degradation [29]. TGA curves show the first weight loss of MCC and NCC at the range 24 - 130 °C temperature due to removal of moisture. But the increasing of mass within the temperature range 20 - 220 °C may be due to the interaction of the sample with that of the TGA medium (TGA analyzer) like nitrogen (N<sub>2</sub>). Another probable reason behind this mass gain may

be the Archimedes effect. The further degradation is occurred at the range of 171 - 270 °C. Abraham *et al.* stated that hemicelluloses started its decomposition at 220 °C and continued up to 300 °C. The decomposition peak reached the maximum weight loss at 268 °C showing a 20 wt. % of solid residuals at 700 °C. Finally, they showed that lignin decomposition extended to the whole temperature range starting below 200 °C and persisting above 700 °C. The solid residue left from lignin pyrolysis was the highest one, 46 wt. % [37]. Acid treated CLC i.e. MCC and NCC showed very trace weight loss. These values proved that acid treated CLC have very minor quantity of hemicellulose and lignin. However, raw CLC showed huge weight loss at the temperature range of 220 - 300 °C. This weight loss may be due to the degradation of low molecular weight fraction of carbohydrates. The final degradation is occurred at the range of 271 - 400 °C and respective weight loss is due to degradation of cellulose. Yang *et al.* showed that in the thermal analysis, cellulose decomposition started at 310 °C and persisted until 400 °C [39].

The DTG curves are the differential form of TG curves. The peaks reveal the different stages of degradation of different CLC, MCC and NCC. Therefore, the thermal stability of the MCC is better than that of NCC. The possible reason behind this observation is that the MCC has higher crystallinity as compared with the NCC which is previously confirmed by XRD analysis.

#### 4. CONCLUSIONS

From the present study, the bulk density of MCC and NCC has been increased than those of raw and bleached CLC samples. On acid hydrolysis, the hydroxyl group of CLC is oxidized to aldehyde or carboxylic acid group thus gives the identical peak at 1736 cm<sup>-1</sup>. As the concentration of acid increases, the intensity of the peak at 1736 cm<sup>-1</sup> of the NCC increases. From the SEM images of different samples it is found that the surface roughness is increased by the acid treatment. On the analysis of TGA and DTG, it is found that the thermal stability is increased for chemical treatment and crystallinity index is also increased. The thermal stability of MCC is better than that of NCC. Moreover, the diffraction intensity of relative diffraction angle is increased after acid hydrolysis. Thus the practical approach of MCC and NCC could be a potential, cost effective and eco-friendly method.

**Acknowledgements.** We hereby acknowledge the assistance of the Chairman of Bangladesh Council for Scientific and Industrial Research (BCSIR), Dhaka, Bangladesh for instrumental measurements through the research work.

**CrediT authorship contribution statement.** M.S.P.: Methodology, Investigation. S.M.A.R.: Formal analysis, Supervision. G.M.A.K.: Formal analysis, Draft preparation, Revision. M.S.A.: Funding acquisition. M.R.: Formal analysis, Supervision.

**Declaration of competing interest.** We are declared that we have no known competing financial interests or personal relationships that could have appeared to influence the work reported in this paper.

#### REFERENCES

1. Gray D. G. – Recent advances in chiral nematics structure and iridescent color of cellulose nanocrystals films. *Nanomater.* **6** (2016) 213-221. Doi: [10.3390/nano6110213](https://doi.org/10.3390/nano6110213)
2. Khalil H. P. S. A., Aprilia N. A. S., Bhat A. H., Jawaid M., Paridah M. T., Rudi D. – A Jatropha biomass as renewable materials for biocomposites and its applications. *Ren. & Sust. Ene. Rev.* **22** (2013) 667-685. Doi: [10.1016/j.rser.2012.12.036](https://doi.org/10.1016/j.rser.2012.12.036)

3. Poletto M., Pistor V., Zattera A. J. – Structural Characteristics and Thermal Properties of Native Cellulose. *Cellul. Fundam. Asp.* (2013) 45-68. Doi.org/10.5772/50452
4. Wegner T. H., Jones P. E. – Advancing cellulose-based nanotechnology. *Cellu.* **13** (2006) 115-118. Doi:10.1007/s10570-006-9056-1
5. de Moraes T. E., Corrêa A. C., Manzoli A., de Lima L. F, Ribeiro de Oliveira C., Capparelli Mattoso L. H. – Cellulose nanofibers from white and naturally colored cotton fibers. *Cellu.* **17** (2010) 595-606. Doi:10.1007/s10570-010-9403-0
6. Sczostak A. – Cotton linters: An alternative cellulosic raw material. *Macromol. Sympo.* **280** (2009) 45-53. doi.org/10.1002/masy.200950606
7. Rahman M., Arifuzzaman Khan G. M., Abdur Razzaque S. M., Ahsanul Haque M., Gafur M. A., Shamsul Alam M. – Fabrication and mechanical/thermal properties of composites from cotton linter and urea formaldehyde resin. *Indian Jour. Of Fib. & Tex. Res.* **47** (2022) 326-333. Doi:10.56042/ijftr.v47i3.51398
8. Ding C., Zhu X., Ma X., Yang H. – Synthesis and Performance of a Novel Cotton Linter Based Cellulose Derivatives Dispersant for Coal-Water Slurries. *Poly.* **14** (2022) 1103. doi.org/10.3390/polym14061103
9. Wang Q., Zhu J. Y., Considine J. M. – Strong and optically transparent films prepared using cellulosic solid residue recovered from cellulose nanocrystals production waste stream. *ACS Appl Mater Interfaces* **5** (2013) 2527-2534. Doi:10.1021/am302967m
10. Choi Y. J., Simonsen J. - Cellulose nanocrystal-filled carboxymethyl cellulose nanocomposites. *Jour. of Nano. & Nanotech.* **6** (3) (2006) 633-639. Doi:10.1166/jnn.2006.132
11. Mandal A., Chakrabarty D. - Isolation of nanocellulose from waste sugarcane bagasse (SCB) and its characterization. *Carbohy. Poly.* **86** (2011) 1291-1299. DOI:10.1016/j.carbpol.2011.06.030
12. Abraham E., Deepa B., Pothan L. A., Jacob M., Thomas S., Cvelbar U., Anandjiwala R. - Extraction of nanocellulose fibrils from lignocellulosic fibres a novel approach. *Carbohy. Poly.* **86** (2011) 1468-1475. Doi:10.1016/j.carbpol.2011.06.034
13. Zhao H. P., Feng X. Q., Gao, H. - Ultrasonic technique for extracting nanofibers from nature materials. *Appl. Phys. Lett.* **90** (2007) 073112. Doi:10.1063/1.2450666
14. Paakko M., Ankerfors M., Kosonen H., Nykanen A., Ahola, S., Osterberg M. - Enzymatic hydrolysis combined with mechanical shearing and high-pressure homogenization for nanoscale cellulose fibrils and strong gels. *Biomacromoi.* **8** (2007) 1934-1941. Doi:10.1021/bm061215p
15. Cheng Q., Wang S., Rials T. – Poly (vinyl alcohol) nanocomposites reinforced with cellulose fibrils isolated by high intensity ultrasonication. *Composites part A: App. Sci. and Manufac.* **40** (2009) 218-224. Doi:10.1016/j.compositesa.2008.11.009
16. Capadona J. R., Shanmuganathan K., Trittschuh S., Seidel S., Rowan S. J., Weder C. - Polymer nanocomposites with nanowiskers isolated from microcrystalline cellulose. *Biomacromol.* **10** (2009) 712–716. Doi: 10.1021/bm8010903.
17. Eichhorn S. J., Dufresne A., Aranguren M., Marcovich N. E., Capadona J. R., Rowan S. J et

- al. - Review: Current international research into cellulose nanofibres and nanocomposites. *J. of Mat. Sci.* **45** (2010) 1–33. <https://doi.org/10.1007/s10853-009-3874-0>
18. Stelte W., Sanadi A. - Preparation and characterization of cellulose nanofibers from two commercial hardwood and softwood pulps. *Indus. & Eng. Chem. Res.* **48** (2009) 11211–11219. Doi: 10.1021/ie9011672
19. Teixeira E., Corrêa A. C., Manzoli A., Leite F. L., Oliveira C. R., Mattoso L. H. C. - Cellulose nanofibers from white and naturally colored cotton fibers. *Cellu.* **17** (2010) 595–606. Doi: 10.1007/s10570-010-9403-0
20. Oksman K., Mathew A. P., Bondeson D., Kvien I. - Manufacturing process of cellulose whiskers/polylactic acid nanocomposites. *Compos. Sci. Technol.* **66** (2006) 2776. Doi:10.1016/j.compscitech.2006.03.002
21. Qua E. H., Hornsby P. R., Sharma H. S. S., Lyons G., McCall R. D. - Preparation and characterization of poly (vinyl alcohol) nanocomposites made from cellulose nanofibers. *Jou. Appl. Polym. Sci.* **113** (2009) 2238. <https://doi.org/10.1002/app.30116>
22. Ge H., Zhang L., Xu M., Cao J., Kang C. - Preparation of di-aldehyde cellulose and its antibacterial activity, in advances in applied aiotechnology, ICAB 2016. Lecture Notes in Electrical Engineering, edited by H Liu, C Song and A Ram. Vol. 444 (Springer, Singapore) 2016.
23. Janovsky A. C., McCredia E. J., Janet E. - Chemical Abstract **123** (2005) 114360 z.
24. Ono S., Keiko K. - Kokai Tokkya Koho. JP Patent 07 143 856 (1995).
25. Wei L., Xin Z., Shouxin L. - Preparation of entangled nanocellulose fibers from APMP and its magnetic functional property as matrix. *Carbohy. Poly.* **94** (2013) 278-285. Doi:10.1016/j.carbpol.2013.01.052
26. Eichhorn S. J., Dufresne A., Aranguren M., Marcovich N. E., Capadona J. R., Rowan S. J. *et al.* - Review: current international research into cellulose nanofibres and nanocomposites. *Jour. Mater. Sci.* **45** (2010) 1-33. Doi:10.1007/s10853-009-3874-0
27. Bharimalla A. K., Deshmukh S. P., Patil S., Nadanathangam V., Saxena S. - Development of energy efficient nanocellulose production process by enzymatic pretreatment and controlled temperature refining of cotton linters. *Cellu.* **30** (2022) 833-847. Doi:10.1007/s10570-022-04959-y
28. Abraham E., Deepa B., Pothan L. A., Jacob M., Thomas S., Cvelbar U., Anandjiwala R. - Extraction of nanocellulose fibrils from lignocellulosic fibers: A novel approach. *Carbohy. Poly.* **86** (2011) 1468-1475. <https://doi.org/10.1016/j.carbpol.2011.06.034>
29. Singanusong R., Tochampa W., Kongbangkerd T., Sodchit C. - Extraction and Properties of Cellulose from Banana Peels. *Jour. of Sci. and Technol.* **21** (2014) 201-213. Doi:10.14456/sjst.2014.16
30. Prakhongpan T., Nitithamyong A., Luanpituksa P. - Extraction and application of dietary fiber and cellulose from pineapple cores. *Jour. of Food Scien.* **67** (2006) 1308-1313. Doi:10.1111/j.1365-2621.2002.tb10279.x
31. Lojewska J., Miskoeiec P., Lojewski T., Pronienwicz L. M. - Cellulose oxidative and hydrolytic degradation: In situ FTIR approach. *Polymer Degradation and Stability* **88** (2005) 512-520. Doi:10.1016/j.polymdegradstab.2004.12.012
32. Mwaikambo Y., Ansell M. P. - The effect of chemical treatment on the properties of hemp,

- sisal, jute and kapok fibers for composite reinforcement. *Appl. Macromol. Chem. and Phys.* **272** (1999) 108-116. Doi:10.1002/(SICI)1522-9505(19991201)272:1%3C108::AID-APMC108%3E3.0.CO;2-9
33. Yasmin Priya S., Arifuzzaman Khan G. M., Helal Uddin M., Ahsanul Haque M., Shaharul Islam M., Abdullah-Al-Mamun M., Gafur M. A., Shamsul Alam M. - Characterization of Micro-fibrillated Cellulose Produced from Sawmill Wastage: Crystallinity and Thermal Properties. *Ame. Chem. Sci. Jour.* **9** (2015) 1-8. Doi:10.9734/ACSIJ/2015/19752
34. Bhariamalla A. K., Patil P. G., Deshmukh S. P., Vigneshwaran N. - Energy efficient production of nano-fibrillated cellulose (NFC) from cotton linters by tri-disc refining and its characterization. *Cellu. Chem. and Tech.* **51** (2017) 395-401. [http://www.cellulosechemtechnol.ro/pdf/CCT5-6\(2017\)/p.395-401.pdf](http://www.cellulosechemtechnol.ro/pdf/CCT5-6(2017)/p.395-401.pdf)
35. Shahpar D. S. - Environmental Compliance Opportunities in the Bangladeshi Ready Made Garments Industry: Lessons from the Green High Achievers, September, (2018). <https://www.greenpolicyplatform.org/sites/default/files/downloads/resource/EDGG+Paper+8+Green+Compliance+in+RMG.pdf>
36. Wu S., Tang Z., Jiang Z., Yu Z., Wang L., Preparation and characterization of hydrophobic cotton fiber for water/oil separation by electrolysis plating combined with chemical corrosion. *Inter. Res. Jou. of Pub. and Envi. Health* **2** (2015) 144-150. <http://dx.doi.org/10.15739/irjpeh.032>
37. Park S., Baker J. O., Himmel M. E., Parilla P. A., Johnson D. K. - Cellulose Crystallinity Index: measurement techniques and their impact on interpreting cellulose performance. *Biotech. for Biofu.* **3** (2010) 1-10. Doi: 10.1186/1754-6834-3-10
38. Kanchanalai P., Temani G., Kawajiri Y., Matthew J. R. - Reaction Kinetics of Concentration Acid Hydrolysis for Cellulose and Hemicellulose and Effect of Crystallinity. *Bio-Reso.* **11** (2016) 1672-1689. Doi:10.15376/biores.11.1.1672-1689
39. Yang H., Yan R., Dong H. L., Zheng C. - Characteristics of hemicelluloses, cellulose and lignin pyrolysis. *Fuel* **86** (2007) 1781-1788. Doi:10.1016/j.fuel.2006.12.013